Using satellite radar backscatter to predict above-ground woody biomass: A consistent relationship across four different African landscapes

E. T. A. Mitchard,[1] S. S. Saatchi,[2] I. H. Woodhouse,[1] G. Nangendo,[3] N. S. Ribeiro,[4] M. Williams,[1] C. M. Ryan,[1] S. L. Lewis,[5] T. R. Feldpausch,[5] and P. Meir[1]

Received 16 September 2009; revised 26 October 2009; accepted 2 November 2009; published 2 December 2009.

[1] Regional-scale above-ground biomass (AGB) estimates of tropical savannas and woodlands are highly uncertain, despite their global importance for ecosystems services and as carbon stores. In response, we collated field inventory data from 253 plots at four study sites in Cameroon, Uganda and Mozambique, and examined the relationships between field-measured AGB and cross-polarized radar backscatter values derived from ALOS PALSAR, an L-band satellite sensor. The relationships were highly significant, similar among sites, and displayed high prediction accuracies up to 150 Mg ha^{-1} (±∼20%). AGB predictions for any given site obtained using equations derived from data from only the other three sites generated only small increases in error. The results suggest that a widely applicable general relationship exists between AGB and L-band backscatter for lower-biomass tropical woody vegetation. This relationship allows regional-scale AGB estimation, required for example by planned REDD (Reducing Emissions from Deforestation and Degradation) schemes.
Citation: Mitchard, E. T. A., S. S. Saatchi, I. H. Woodhouse, G. Nangendo, N. S. Ribeiro, M. Williams, C. M. Ryan, S. L. Lewis, T. R. Feldpausch, and P. Meir (2009), Using satellite radar backscatter to predict above-ground woody biomass: A consistent relationship across four different African landscapes, *Geophys. Res. Lett.*, *36*, L23401, doi:10.1029/2009GL040692.

1. Introduction

[2] There is no universally accepted methodology for assessing the above-ground biomass (AGB) of woody tropical landscapes. While there is a degree of consensus on the best methods of collecting ground-based inventory data [*Brown*, 1997; *Chave et al.*, 2009; *Phillips et al.*, 2009], and a general agreement that remote sensing data provides the best methodology for both scaling-up ground-based measurements and monitoring changes over large scales, there is a plethora of different sensors and analytical procedures available for scaling-up AGB estimates [*Lu*, 2006].

[3] Tropical savanna and woodland ecosystems provide substantial ecosystem services at local to global scales: the provision of timber, fuel and other products, the regulation of soil and water, biodiversity retention, atmospheric services and eco-tourism. However, attempts to mitigate rising atmospheric CO_2 levels have led to projects aiming to preserve these ecosystems based solely on their carbon stocks. To be successful, whether in voluntary carbon markets or via a post-Kyoto climate change agreement under one of the Reducing Emissions from Deforestation and Degradation (REDD) frameworks, a universal, low-cost and robust way to measure and monitor carbon stocks over large regions is needed [*Grassi et al.*, 2008].

[4] An ideal large-scale AGB measurement system would be one that could sense AGB directly, and as such would have no upper biomass limit, and do so independently of cloud cover. Currently no such system exists, although future satellite platforms which will combine fully polarimetric radar with measurements of vegetation height may come closer to this goal [*Donnellan et al.*, 2008; *Le Toan et al.*, 2008]. However, for areas with an AGB < ∼150 Mg ha^{-1}, which incorporates the savanna and woodland biomes, and drier tropical forest formations, the L-band radar sensor ALOS PALSAR may go some way towards providing a system for measuring AGB that meets observational requirements. In this paper we set out evidence supporting this claim.

[5] Synthetic Aperture Radar (SAR) sensors are active instruments, sending a pulse of microwave radiation and detecting the radiation scattered back (backscatter, referred to as sigma0 [σ^0]) by the surface and the 3-dimensional structures on it. When longer wavelength microwaves are used (>20 cm) the detected radiation is mostly due to backscattering from the branching elements and stems of the trees, and thus radar should respond in a characteristic way to forest volume and biomass [*Saatchi and Moghaddam*, 2000]. As a result, long wavelength SAR has a stronger and more universal relationship than optical or short wavelength microwave sensors which are sensitive to leaf characteristics, where relationships with the woody component of vegetation are indirect and thus highly site- and season- specific. The radar backscatter response saturates at higher biomass values in savanna ecosystems, at a variable point (>60 Mg ha^{-1} [*Santos et al.*, 2002], >80 Mg ha^{-1} [*Lucas et al.*, 2000], and >150 Mg ha^{-1} [*Mitchard et al.*, 2009], all using different L-band systems). This saturation point is due to the competing mechanisms of scattering and attenuation (absorption) of microwave energy in the canopy of the vegetation, and is highly dependent on the canopy density, stem density, tree species, and vegetation and soil moisture conditions, as well as the characteristics of the radar data used. Nevertheless, this point is high enough that useful biomass

[1]School of Geosciences, University of Edinburgh, Edinburgh, UK.
[2]Jet Propulsion Laboratory, California Institute of Technology, Pasadena, California, USA.
[3]Wildlife Conservation Society, Kampala, Uganda.
[4]Faculdade de Agronomia e Engenharia Florestal, Universidade Eduardo Mondlane, Maputo, Mozambique.
[5]Earth and Biosphere Institute, School of Geography, University of Leeds, Leeds, UK.

0094-8276/09/2009GL040692

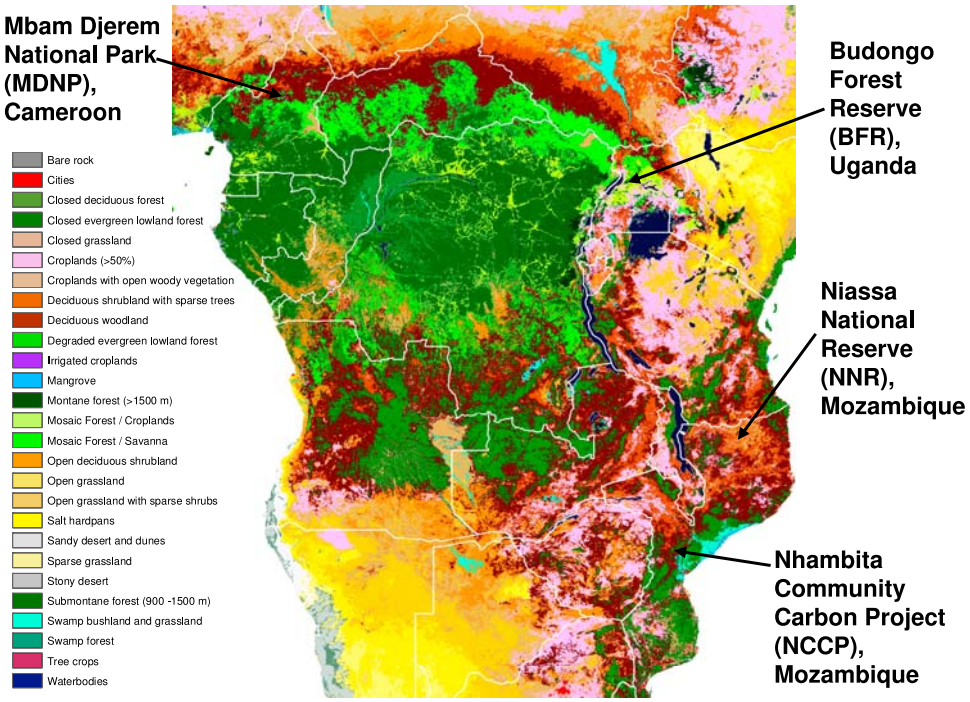

Figure 1. The location of the field sites is shown on a landcover map for the year 2000 produced by *Mayaux et al.* [2004].

estimates are possible for mixed tree-grass systems (savannas and woodlands), as these typically have maximum AGB values <100 Mg ha^{-1}, though higher values can exist in gallery forests [*Brown*, 1997].

[6] Advanced Land Observing Satellite (ALOS) Phased Array L-band Synthetic Aperture Radar (PALSAR) was launched in January 2006. It operates at a 23.6 cm wavelength in a number of modes, but the Fine-beam dual-polarization (FBD) mode, which provides HH (horizontal transmit and horizontal receive) and HV (horizontal transmit and vertical receive) data at a 34.3° incidence angle, shows the greatest potential for these purposes. This is because of its high signal:noise ratio, high resolution (~20 m), provision of cross-polarized data, and because it is being systematically collected across the tropics with the aim of forming a freely-available 50 m resolution mosaic (http://www.eorc.jaxa.jp/ALOS/en/kc_mosaic/kc_mosaic.htm).

[7] PALSAR, and other L-band systems, have previously been shown to respond to the AGB of tropical savannas and woodlands with varying degrees of accuracy [*Lucas et al.*, 2000; *Mitchard et al.*, 2009; *Podest and Saatchi*, 2002; *Santos et al.*, 2002]. However, in these studies the field datasets were small and from one geographic area. Here we examine the PALSAR response to AGB at four different intensively sampled locations across tropical Africa to test the consistency of the relationship between backscatter and AGB. We then examine the efficacy of models derived from three sites to predict the AGB of measured plots in a fourth site, thus providing a much better test of the utility of such data for assessing AGB than has previously been performed.

2. Data and Methods

2.1. Field Data

[8] The field sites were located in Cameroon, Uganda and Mozambique (Figure 1); in all cases standardized forestry methodologies were employed. Diameters of all stems >10 cm diameter at breast height (DBH) were measured and their species recorded; height was also measured for ~30% of stems in the Cameroon and Uganda sites using vertex hypsometers (Haglöf, Sweden). None of the study areas exhibit steeply dissected topography.

2.1.1. Mbam Djerem National Park (MDNP), Cameroon

[9] MDNP encompasses the transition between savanna and forest contiguous with the Congo Basin. Eight 1 ha square plots and ten 0.4 ha transects (8 × 20 m × 200 m & 2 × 40 m × 100 m) in forest and savanna regions in three areas of the park near 6°9′N, 12°50′E were sampled in 2007, with AGB ranging from 6 – 418 Mg ha^{-1} [*Mitchard et al.*, 2009]. Transects that covered both forest and savanna were split into two data-points, giving 24 points in total.

2.1.2. Budongo Forest Reserve (BFR), Uganda

[10] BFR is a remnant patch of tropical forest surrounded by farmland to the south and east, and savanna to the west and north. One 1.86 ha square plot and eleven 0.5 ha transects (20 m × 250 m) were measured in 2008 by E. Mitchard, and 261 × 0.04 ha & 335 × 0.05 ha circular plots in the savannas and woodlands to the north of the reserve were measured in 2001 [*Nangendo et al.*, 2005]; these latter plots are small and highly clustered, and as such were averaged in groups of 5–6 within 100 m × 100 m areas, giving a total of 118 data points (0.2 – 0.3 ha). AGB ranged from 6 – 876 Mg ha^{-1}, with the plots near 1°52′N, 31°39′E.

2.1.3. Niassa National Reserve (NNR), Mozambique

[11] NNR is a 23 000 km^2 protected area in the north of Mozambique, dominated by Miombo woodland, with the woody fraction of vegetation increasing in density from East to West due to a rainfall and disturbance gradient. Fifty 0.07 ha circular plots distributed across the park were

measured in 2004 [*Ribeiro et al.*, 2008] around 12°2′S, 37°15′E. ALOS PALSAR scenes were available for 42, ranging in AGB from 2–41 Mg ha^{-1}.

2.1.4. Nhambita Community Carbon Project (NCCP), Mozambique

[12] NCCP is an area of Miombo woodland in central Mozambique. It has more influence from humans and is more regularly burnt than NNR, and has different dominant species. Data were collected for thirteen 1 ha square plots, five 0.5 ha circular plots, and thirty-eight 0.25 ha square plots in 2004-7, with an AGB of 3–120 Mg ha^{-1}, near 18°57′S, 34°9′E [*Williams et al.*, 2008].

2.2. Conversion to AGB

[13] Field plot data were converted to AGB using the best available methods for each vegetation type. For MDNP and BFR no local allometry data exist, so the *Chave et al.* [2005] pan-tropical optimum allometric equations were used, using wood density, height and DBH. The moist tropical forest equation was used for forest species, and the dry forest equation for savanna species. Height was measured for ~30% of the stems and used to develop site-specific height-DBH relationships to obtain AGB [*Mitchard et al.*, 2009]. Wood density data were taken from the Global Wood Density Database [*Chave et al.*, 2009]; where species-specific data was not present, the average value for African members of the same genus were used. For NNR an allometric equation involving DBH alone was used, derived from similar vegetation and climatic conditions nearby in Tanzania, taken from *Mugasha and Chamshama* [2002]. For NCCP destructive sampling was performed to produce a site-specific allometric relationship [*Ryan*, 2009]. All plot AGB values were then converted to Mg ha^{-1}; it should be noted that these values are dry AGB, not carbon content, and exclude woody stems < 10 cm, shrubs, grasses, below-ground sources and necromass. This exclusion of other above-ground vegetation will cause an underestimate of AGB of ~5% for forest and dense woody savanna plots [*Mitchard et al.*, 2009], and the size of this error will increase for lower biomass plots (it is 12% for NCCP [*Ryan*, 2009]). However, the derivation from field data of a local correction factor should be sufficient to correct for this, as L-band radar will respond mostly to larger stems [*Collins et al.*, 2009].

2.3. SAR Data

[14] L-band dual-polarization (HH/HV) satellite radar data from the ALOS PALSAR sensor in the FBD mode were acquired over all field sites from 2007 (see Table S1 of the auxiliary material for scene IDs and dates)[1]. The data were provided at a 12.5 m pixel spacing (4 looks per pixel), and were converted from digital number to sigma0 using the revised calibration coefficients [*Shimada et al.*, 2009]. The scenes were warped to Landsat ETM+ data covering the areas of the field sites, using observable common features such as islands, road junctions, and permanent vegetation features, with a Root Mean Square Error (RMSE) always <0.6 Landsat pixels (18 m), and the backscatter values for pixels covering each field site extracted, with pixels averaged in the power domain so the arithmetic, not geometric, means were used. This type of warping is only possible because all the study areas have little significant topography, so the problem of layover (where topographic features are distorted, bending towards the sensor) is minimized. After averaging, power values were converted back to sigma0 before being regressed against AGB. All remote sensing analyses were performed using ENVI 4.6 (ITT, Boulder, USA), and all regression analyses with Sigmaplot 11.0 (Systat, Chicago, USA).

3. Results

3.1. Plot Level AGB-Backscatter Relationships

[15] Strong relationships between AGB and HV backscatter were found at each of the four landscapes (r^2 0.61 – 0.76, $p < 0.0001$), with a clear reduction in sensitivity (saturation) obvious between 150 and 200 Mg ha^{-1}; relationships with the HH polarization were less consistent, though significant positive relationships were still observable in all cases (Figure S1 and Table S2 of the auxiliary material).[1] The fitted models were of the form:

$$\sigma^0 = a + b.\ln(B_{AG}) \quad (1)$$

$$\sigma^0 = a + b.\ln(B_{AG}) + c.(\ln(B_{AG}))^2 \quad (2)$$

Where σ^0 is the sigma0 in decibels, B_{AG} is the AGB in Mg ha^{-1}, and a, b and c are constants. Both models were fitted to the observed data, with equation (2) being preferred if the log-squared term was significantly different from zero. These models were chosen as they produced the highest r^2 and lowest RMSE values of a number of simple models tested. Coefficients and uncertainties are shown in Table S2.

3.2. Combined AGB-Backscatter Relationships

[16] Combining the HV sigma0 and AGB values of all four datasets produced a strong relationship, with an r^2 of 0.73 and $p < 0.0001$ using equation (2), and with some sensitivity clearly still present in the data up to 150–200 Mg ha^{-1} (Figure 2b). There was also a significant relationship with HH ($r^2 = 0.56$, $p < 0.0001$), but this was less consistent, with saturation occurring at 50–100 Mg ha^{-1} (Figure 2a). The HV relationship fitted was:

$$\sigma^0_{HV} = -22 + 2.73\ln(AGB) - 0.156(\ln(AGB))^2 \quad (3)$$

which rearranged to:

$$AGB = EXP\left[\frac{-2.73 + \sqrt{7.45 - \left(0.623\left(22 + \sigma^0_{HV}\right)\right)}}{-0.311}\right] \quad (4)$$

allows the prediction of AGB from sigma0 values (Figure S2). Attempts were made to combine HH and HV data in a general linear model, but the HH terms were never significant once the HV terms had been taken into account.

3.3. Testing Consistency

[17] The consistency of the general relationship described above was tested using the four independent datasets. For each of the four sites, AGB predictions and resultant RMSE values were calculated using the site-specific HV equations

[1]Auxiliary materials are available in the HTML. doi:10.1029/2009GL040692.

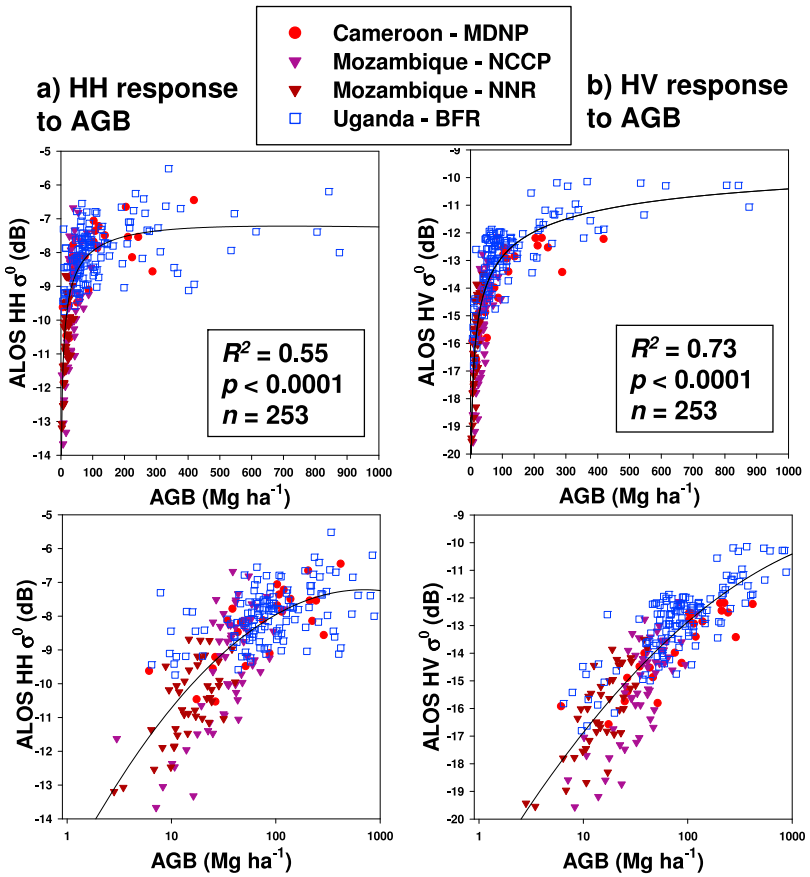

Figure 2. ALOS PALSAR (a) HH and (b) HV backscatter (σ^0) are plotted against field-measured AGB (Mg ha^{-1}) for all four sites combined, with the x-axes shown with conventional and $\log_{10}$ scales. Second order log regression lines are fitted.

(Figure S1 and Table S2). New equations were then calculated using equations derived from the other three datasets only, and predictions made again using the HV values. Both field and predicted values were limited at 400 Mg ha^{-1}, as all possible sensitivity to AGB will be lost by this point, and thus making predictions at such high AGB values has no validity. Predictions for each site obtained by using an equation developed from the three other sites increased the RMSE by only 12–30%, and particularly for data points with AGB < 150 Mg ha^{-1} the RMSE values remained low (Table 1). The average AGB predicted using site-specific equations was within 30% of the field-derived average AGB values, and this error increased negligibly when the equations derived from the other three sites were used (Table 1). However, as the biomass estimation error from radar depends on the errors associated with both radar and ground measurements, the true errors could be greater [*Mitchard et al.*, 2009].

4. Discussion

[18] We have found that PALSAR HV backscatter responds strongly to AGB in a consistent manner across four African sites widely separated in space and differing greatly in their vegetation structure. The relationship derived does contain significant prediction errors (±∼20% for plots <150 Mg ha^{-1}). These are partly because L-band SAR does not respond directly to AGB, but to aspects of vegetation structure [*Saatchi and Moghaddam*, 2000], partially due to spatial variability in structure [*Saatchi et al.*, 2009], and partially due to radar calibration and orthorectification [*van Zyl*, 1990] and field estimation errors propagating through the analysis [*Chave et al.*, 2004]. In addition,

Table 1. Average AGB and RMSE for Field Plots Predicted From HV Data and a Site-Specific Model Versus a Model Derived From the Three Other Sites[a]

		Average AGB (Mg ha^{-1})			RMSE (Mg ha^{-1})		RMSE for Points < 150 Mg ha^{-1}	
Site	*n*	Ground Data	Site-Specific	Other-Three	Site-Specific	Other-Three	Site-Specific	Other-Three
MDNP Cameroon	24	114.7	115.5	82.1	61.5	67.5	37.4	22.3
BFR Uganda	129	137.2	176.8	174.0	67.1	74.9	48.8	69.42
NNR Mozambique	42	17.28	19.0	20.2	8.3	12.8	8.3	12.8
NCCP Mozambique	58	40.7	44.6	37.1	19.2	25.2	19.2	25.2

[a]All AGB values were limited at 400 Mg ha^{-1}

backscatter responds differently to differing soil and vegetation moisture conditions, and the surface topography, adding to observed prediction errors. For a detailed discussion of the errors and uncertainties involved in this type of analysis see *Mitchard et al.* [2009]. Despite these factors, our analysis shows that AGB can be predicted using radar data for large areas dominated by differing vegetation types with useful accuracy. Notably, errors do not increase dramatically when a continental PALSAR HV-AGB equation, rather than one based on local biomass plots, is used to estimate local AGB.

[19] The better relationship between AGB and the HV rather than HH polarization, and its higher congruence among sites, is to be expected, as this polarization is much less influenced by soil and vegetation moisture than HH [*Collins et al.*, 2009]. HV is also less influenced by topography [*van Zyl*, 1993], though in areas of substantial topographical change significant inaccuracies in estimation and geolocation will still arise.

[20] These results have a higher saturation point and less noise than found in previous studies using L-band HV data, [e.g., *Lucas et al.*, 2000; *Santos et al.*, 2002; *Viergever et al.*, 2007]. This could be due to structural features of African savannas, or that the data were acquired during the dry season where errors associated with moisture are minimized. Moreover, FBD data is collected at a low incidence angle (34.3°) compared to airborne radar sensors used by the above studies, allowing the radar signal to penetrate deeper into the vegetation canopy. This, in turn, improves the sensitivity of HV backscatter to AGB and reduces the sensitivity of HH backscatter to AGB because of impacts of soil moisture and roughness. The large number of good quality, well-geolocated field plots in relatively flat areas that were obtained for this study could also be a factor, producing more accurate results than other studies by increasing the signal-to-noise ratio.

[21] When applying equation (4) to any PALSAR scene over African woodlands and savannas errors of 20–30% are to be expected (Table 1), probably increasing by another 10% when uncertainties in allometries are included [*Chave et al.*, 2004; *Williams et al.*, 2008]. Local calibration with a network of field plots will remain essential at least for validation, and for estimating a 'correction factor' for adding the AGB of grasses and stems <10 cm. However, this finding of a consistent response to AGB in these widely separated and quite different ecosystems from an operational satellite SAR sensor offers the potential of rapid, accurate, high resolution, and low cost mapping of the lower biomass woody vegetation of Africa, and potentially other regions in the world. Moreover, the 46-day repeat cycle will allow sufficient images to be captured during the year to negate any effects of seasonality and soil moisture, and allow the monitoring of landscapes for any changes in AGB. This finding suggests that utilization of PALSAR data should be essential for projects involving the mapping and monitoring of woodland and savanna biomass, thus having important implications for carbon-credit projects, such as those under proposed REDD schemes.

[22] **Acknowledgments.** JAXA, ASF, and USGS provided remote sensing data. E Mitchard is funded by Gatsby Plants, and Cameroon fieldwork was also funded by TROBIT, a NERC-funded consortium, and assisted by WCS Cameroon and Bonaventure Sonké. Kirsty Laughlin assisted with data collection in BFR, where the Budongo Conservation Field Station provided local support. C Ryan was funded by NERC and data collection for NCCP was part-funded by the EU, and assisted by Envirotrade Ltd. N Ribeiro acknowledges the Eduardo Mondlane University – Department of forest engineering, IUCN-Mozambique and SGDRN (Sociedade para Gestao e Desenvolvimento da Reserva do Niassa). S Lewis is funded by a Royal Society Research Fellowship. Jon Lloyd provided help and expertise.

References

Brown, S. (1997), Estimating biomass and biomass change of tropical forests, *FAO For. Pap. 134*, Food and Agric. Organ. of the U. N., Rome.

Chave, J., R. Condit, S. Aguilar, A. Hernandez, S. Lao, and R. Perez (2004), Error propagation and scaling for tropical forest biomass estimates, *Philos. Trans. R. Soc. London, Ser. B*, *359*(1443), 409–420, doi:10.1098/rstb.2003.1425.

Chave, J., et al. (2005), Tree allometry and improved estimation of carbon stocks and balance in tropical forests, *Oecologia*, *145*(1), 87–99, doi:10.1007/s00442-005-0100-x.

Chave, J., D. Coomes, S. Jansen, S. L. Lewis, N. G. Swenson, and A. E. Zanne (2009), Towards a worldwide wood economics spectrum, *Ecol. Lett.*, *12*(4), 351–366, doi:10.1111/j.1461-0248.2009.01285.x.

Collins, J. N., L. B. Hutley, R. J. Williams, G. Boggs, D. Bell, and R. Bartolo (2009), Estimating landscape-scale vegetation carbon stocks using airborne multi-frequency polarimetric synthetic aperture radar (SAR) in the savannahs of north Australia, *Int. J. Remote Sens.*, *30*(5), 1141–1159, doi:10.1080/01431160802448935.

Donnellan, A., et al. (2008), Deformation, Ecosystem Structure, and Dynamics of Ice (DESDynI), in *Proceedings of the 2008 IEEE Aerospace Conference*, pp. 163–175, Inst. of Electr. and Electron. Eng., New York.

Grassi, G., S. Monni, S. Federici, F. Achard, and D. Mollicone (2008), Applying the conservativeness principle to REDD to deal with the uncertainties of the estimates, *Environ. Res. Lett.*, *3*(3), 035005, doi:10.1088/1748-9326/3/3/035005.

Le Toan, T., H. Baltzer, P. Paillou, K. Papathanassiou, S. Plummer, S. Quegan, F. Rocca, and L. Ulander (2008), Biomass, in *Candidate Earth Explorer Core Mission*, *Rep. Assess. SP-1313/2*, Eur. Space Agency, Noordwijk, Netherlands.

Lu, D. S. (2006), The potential and challenge of remote sensing-based biomass estimation, *Int. J. Remote Sens.*, *27*(7), 1297–1328, doi:10.1080/01431160500486732.

Lucas, R. M., A. K. Milne, N. Cronin, C. Witte, and R. Denham (2000), The potential of synthetic aperture radar (SAR) for quantifying the biomass of Australia's woodlands, *Rangeland J.*, *22*(1), 124–140, doi:10.1071/RJ0000124.

Mayaux, P., E. Bartholome, S. Fritz, and A. Belward (2004), A new land-cover map of Africa for the year 2000, *J. Biogeogr.*, *31*(6), 861–877, doi:10.1111/j.1365-2699.2004.01073.x.

Mitchard, E. T. A., S. S. Saatchi, I. H. Woodhouse, T. R. Feldpausch, S. L. Lewis, B. Sonké, C. Rowland, and P. Meir (2009), Measuring biomass changes due to woody encroachment and deforestation/degradation in a forest-savanna boundary region of central Africa using multi-temporal L-band radar backscatter, *Remote Sens. Environ.*, in press.

Mugasha, A. G., and S. A. O. Chamshama (2002), Tree biomass and volume estimation for miombo woodlands at Kitulangalo, Morogoro, Tanzania, in *Indicators and Tools for Restoration and Sustainable Management of Forests in East Africa*, *I-TOO Working Pap. 9*, Ethiopian Agric. Res. Cent., Addis Ababa.

Nangendo, G., O. van Straaten, and A. de Gier (2005), Biodiversity conservation through burning: A case study of woodlands in Budongo Forest Reserve, NW Uganda, in *African Forests Between Nature and Livelihood Resources: Interdisciplinary Studies in Conservation and Forest Management*, edited by M. A. Ros-Tonen and T. Dietz, pp. 113–128, Edin Mellen, New York.

Phillips, O. L., T. R. Baker, T. R. Feldpausch, and R. Brienen (2009), Field manual for plot establishment and remeasurement, RAINFOR, Univ. of Leeds, Leeds, U. K. (Available at http://www.geog.leeds.ac.uk/projects/rainfor/)

Podest, E., and S. Saatchi (2002), Application of multiscale texture in classifying JERS-1 radar data over tropical vegetation, *Int. J. Remote Sens.*, *23*(7), 1487–1506, doi:10.1080/01431160110093000.

Ribeiro, N. S., S. S. Saatchi, H. H. Shugart, and R. A. Washington-Allen (2008), Aboveground biomass and leaf area index (LAI) mapping for Niassa Reserve, northern Mozambique, *J. Geophys. Res.*, *113*, G02S02, doi:10.1029/2007JG000550.

Ryan, C. M. (2009), Carbon cycling, fire and phenology in a tropical savanna woodland in Nhambita, Mozambique, Ph.D. thesis, Univ. of Edinburgh, Edinburgh, U. K.

Saatchi, S., and M. Moghaddam (2000), Estimation of crown and stem water content and biomass of boreal forest using polarimetric SAR imagery,

IEEE Trans. Geosci. Remote Sens., *38*(2), 697–709, doi:10.1109/36.841999.

Saatchi, S., M. Marlier, D. Clark, R. Chazdon, and A. Russell (2009), Impact of spatial variability of forest structure on radar estimation of aboveground biomass in tropical forests, *Remote Sens. Environ.*, in press.

Santos, J. R., M. S. P. Lacruz, L. S. Araujo, and M. Keil (2002), Savanna and tropical rainforest biomass estimation and spatialization using JERS-1 data, *Int. J. Remote Sens.*, *23*(7), 1217–1229, doi:10.1080/01431160110092867.

Shimada, M., O. Isoguchi, T. Tadono, and K. Isono (2009), PALSAR radiometric calibration and geometric calibration, *IEEE Trans. Geosci. Remote Sens.*, in press.

van Zyl, J. (1990), Calibration of polarimetric radar images using only image parameters and trihedral corner reflector responses, *IEEE Trans. Geosci. Remote Sens.*, *28*(3), 337–348, doi:10.1109/36.54360.

van Zyl, J. (1993), The effect of topography on radar scattering from vegetated areas, *IEEE Trans. Geosci. Remote Sens.*, *31*(1), 153–160, doi:10.1109/36.210456.

Viergever, K. M., I. H. Woodhouse, and N. Stuart (2007), Backscatter and interferometry for estimating above-ground biomass in tropical savanna woodland, in *IGARSS 2007: IEEE International Geoscience and Remote Sensing Symposium—Sensing and Understanding Our Planet*, pp. 2346–2349, Inst. of Electr. and Electron. Eng., New York.

Williams, M., C. M. Ryan, R. M. Rees, E. Sarnbane, J. Femando, and J. Grace (2008), Carbon sequestration and biodiversity of re-growing miombo woodlands in Mozambique, *For. Ecol. Manage.*, *254*(2), 145–155, doi:10.1016/j.foreco.2007.07.033.

T. R. Feldpausch and S. L. Lewis, Earth and Biosphere Institute, School of Geography, University of Leeds, Leeds LS2 9JT, UK.

P. Meir, E. T. A. Mitchard, C. M. Ryan, M. Williams, and I. H. Woodhouse, School of Geosciences, University of Edinburgh, EH8 9XP, UK. (edward.mitchard@ed.ac.uk)

G. Nangendo, Wildlife Conservation Society, P.O. Box 7487, Kampala, Uganda.

N. S. Ribeiro, Faculdade de Agronomia e Engenharia Florestal, Universidade Eduardo Mondlane, P.O. Box 257, Maputo, Mozambique.

S. S. Saatchi, Jet Propulsion Laboratory, California Institute of Technology, Pasadena, CA 91109, USA.